Space charge studies based on beta measurement in J-PARC MR

K. Ohmi

KEK, Accelerator Lab

Dec. 10, 2015, talk at Fermilab

Overview

Introduction

Particles move with experience of electro-magnetic field of lattice elements and space charge. Slow emittance growth arising in a high intensity circular proton ring is studied.

- We assume that the beam distribution is static, and each particle moves in the filed of the static distribution.
- A halo is formed by the nonlinear force due to the electro-magnetic field of the beam itself.
- The halo, which consists of small part of whole beam, does not affect the electro-magnetic field.
- Particle motion is described by a single particle Hamiltonian in the field.
- This picture is not self-consistent for a distortion of beam distribution due to space charge force.

Practical issue in J-PARC MR; the beam loss of 0.1-1% during $\approx 10,000 - 100,000$ turns.

Real issue: J-PARC MR operating point

Choice of operating point in J-PARC MR.

1. New operating point (21.3,21.4) is better than present one (22.40,20.75) in simulations and experiments.
2. Qualitative understanding of the reasons is necessary.

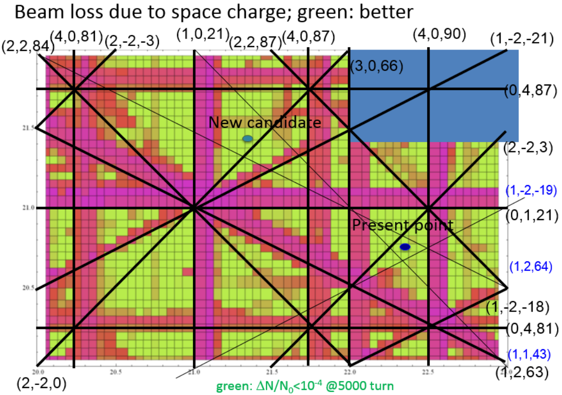

Figure: Tune scan of beam loss in a space charge simulation (SCTR).

Beam loss measureemnt at new operating point (21.23,21.31)

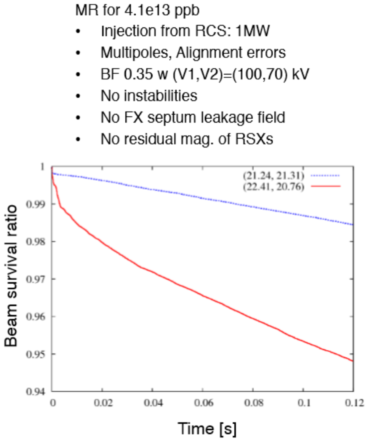

Figure: Measured beam loss at $(\nu_x, \nu_y) = (21.23, 21.31)$.

How high power is expected at new operating point

With two bunches

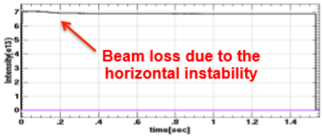

Extracted beam : 3.41e13 ppb
6.82e13 ppp (132 kW eq. ,2 bunches)

	Beam loss[Watt]	
INJ(K1+K2+K3+K4)	144	7.43e+11
P2 --> +90ms	241	1.00e+12
P2+90ms --> +120ms	31	1.30e+11
P2+100ms ---> EXT		1.83e+11

Total beam loss ~ 420 W

Near future tunable knobs to reduce the beam loss:
Injection kicker, BxB feed-back,
2nd harmonic cavity, VHF cavity, etc.

	Bunch number	repetition period (sec)	Beam power (kW)	Beam loss (kW)	Notes
1	2	2.48	132	0.42	measurement
2	8	2.48	529	1.7	estimation
3	8	1.3	1009	3.2	estimation

The MR has capability to reach 1MW with the high repetition rate operation.

Hamiltonian for a particle under the space charge force

Betatron variables with action variable/angle expression.

$$\begin{aligned} x(s) &= \sqrt{2\beta_x(s)J_x}\cos(\phi_x(s)) \\ y(s) &= \sqrt{2\beta_y(s)J_y}\cos(\phi_y(s)). \end{aligned} \quad (1)$$

Hamiltonian, which characterize one turn map, is separated by three parts

- linear betatron motion (μJ)
- nonlinear component of the lattice magnets (U_{nl})
- space charge potential (U).

$$H = \mu J + U_{nl} + U_{sc}. \quad (2)$$

Betatron phase advance per turn,

$$\tilde{\mu}_x = \phi_x(s+L) - \phi_x(s) = \frac{\partial H}{\partial J_x} = \mu_x + \frac{\partial(U_{nl}+U_{sc})}{\partial J_x} \quad (3)$$

Fourier expansion of Hamiltonian

$$H = \mu J + U_{00}(J) + \sum_{m_x, m_y \neq 0} U_{m_x,m_y}(J) \exp(-i m_x \phi_x - i m_y \phi_y) \qquad (4)$$

Tune shift, tune slope

First and second terms in RHS characterize shift, spread and slope of tune.

$$\tilde{\mu}_x = \frac{\partial H}{\partial J_x} = \mu_x + \frac{\partial U_{00}}{\partial J_x} \qquad (5)$$

Resonance

Resonance occurs, when $m_x \tilde{\mu}_x + m_y \tilde{\mu}_y = 2\pi n$ is satisfied at a amplitude $(J_{x,R}, J_{y,R})$; effect of $U_{\boldsymbol{m}}$ is accumulated turn by turn.

Expansion around Resonance

J. L. Tennyson, AIP Conference proceedings, 87, 345 (1982).

Resonance condition

$$m_x\tilde{\mu}_x(J_x,J_y)+m_y\tilde{\mu}_y(J_x,J_y)=2\pi n$$

Above condition gives a fixed point(line) in (J_x,J_y) space for particle motion.

Expansion of Hamiltonian around the fixed point

$$U_{00}(\boldsymbol{J})=U_{00}(\boldsymbol{J}_R)+\left.\frac{\partial U_{00}}{\partial \boldsymbol{J}}\right|_{\boldsymbol{J}_R}(\boldsymbol{J}-\boldsymbol{J}_R)+(\boldsymbol{J}-\boldsymbol{J}_R)^t\frac{1}{2}\left.\frac{\partial^2 U_{00}}{\partial \boldsymbol{J}\partial \boldsymbol{J}}\right|_{\boldsymbol{J}_R}(\boldsymbol{J}-\boldsymbol{J}_R) \tag{6}$$

Tune slope

$$\frac{\partial \nu_i}{\partial J_j}=\frac{\partial \nu_j}{\partial J_i}=\frac{\partial^2 U_{00}}{\partial J_i\partial J_j} \tag{7}$$

Standard Model

Resonance term around the fixed point

$$U_m(\boldsymbol{J}) \approx U_{\boldsymbol{m}}(\boldsymbol{J}_R) \qquad \boldsymbol{m} = (m_x, m_y) \tag{8}$$

Standardized Hamiltonian

$$H = \frac{\Lambda}{2} P_1^2 + U_{\boldsymbol{m}}(\boldsymbol{J}_R) \cos\psi_1 \tag{9}$$

$$\Lambda = m_x^2 \frac{\partial^2 U_{00}}{\partial J_x^2} + m_x m_y \frac{\partial^2 U_{00}}{\partial J_x \partial J_y} + m_y^2 \frac{\partial^2 U_{00}}{\partial J_y^2}$$

Resonance width (full width)

$$\Delta P_1 = 4\sqrt{\frac{U_{\boldsymbol{m}}}{\Lambda}} \qquad \Delta J_x = 4 m_x \sqrt{\frac{U_{\boldsymbol{m}}}{\Lambda}} \tag{10}$$

Standard Model

.

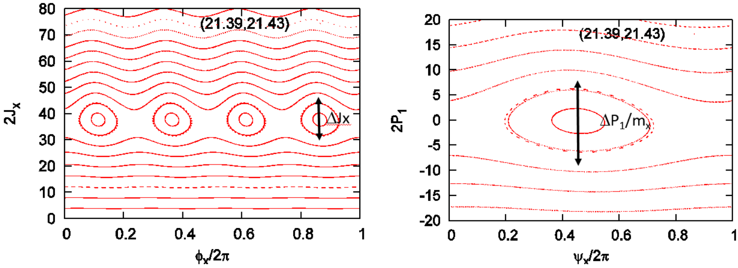

Figure: Relation between (J_x, ϕ_x) and (P_1, ψ_1).

Space Charge Potential

Assume Gaussian beam in x,y,z

$$U_{sc}(s',s) = -\frac{\lambda_p r_p}{\beta^2\gamma^3}\int_0^\infty \frac{1-\exp\left(-\frac{x(s',s)^2}{2\sigma_x^2+u}-\frac{y(s',s)^2}{2\sigma_y^2+u}\right)}{\sqrt{2\sigma_x^2(s')+u}\sqrt{2\sigma_y^2(s')+u}}du \qquad (11)$$

$$\begin{aligned} x(s',s) &= \sqrt{2\beta_x(s')J_x}\cos(\varphi_x(s',s)+\phi_x(s))+\eta(s')\delta(s) \\ y(s',s) &= \sqrt{2\beta_y(s')J_y}\cos(\varphi_y(s',s)+\phi_y(s)). \end{aligned} \qquad (12)$$

where $\varphi_{x,y}(s',s)$ is the betatron phase difference between s and s' and η is the dispersion. $\delta(s)$ is given function of s, not canonical variable.

$$U_{sc}(s) = \oint ds' U_{sc}(s',s) \qquad (13)$$

U_{00}

$$U_{00}(J_x, J_y) = -\frac{\lambda_p r_p}{\beta^2\gamma^3} \oint ds \int_0^\infty \frac{dt}{\sqrt{2+t}\sqrt{2r_{yx}+t}} \tag{14}$$

$$\left[1 - e^{-w_{x\eta}-w_y} \sum_{l=-\infty}^{\infty} (-1)^l I_{l/2}(w_x) I_l(v_x) I_0(w_y)\right].$$

where $t = u/\sigma_x^2$ and $r_{yx} = \sigma_y^2/\sigma_x^2$ and

$$w_x = \frac{\beta_x J_x}{2\sigma_x^2 + u}. \qquad w_{x\eta} = \frac{\beta_x J_x + \eta^2\delta^2}{2\sigma_x^2 + u}. \tag{15}$$

$$v_x = \frac{2\sqrt{2\beta_x J_x}\eta\delta}{2\sigma_x^2 + u} \qquad w_y = \frac{\beta_y J_y}{2\sigma_y^2 + u}. \tag{16}$$

Tune shift Space Charge Potential

$$2\pi\Delta\nu_x = \frac{\partial U_{00}}{\partial J_x} = -\frac{\lambda_p r_p}{\beta^2\gamma^3}\oint ds \frac{\beta_x}{\sigma_x^2}$$
$$\int_0^\infty \frac{e^{-w_x - w_y} dt}{(2+t)^{3/2}(2r_{yx}+t)^{1/2}}\left[(I_0(w_x) - I_1(w_x))I_0(w_y)\right], \qquad (17)$$

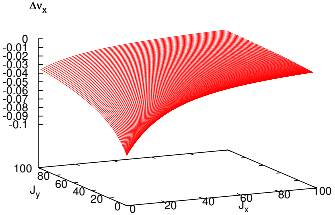

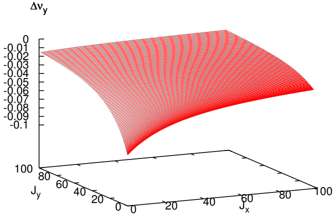

Figure: Tune spread ($\Delta\nu_{x,y}(J_x, J_y)$) due to space charge force.

Tune footprint

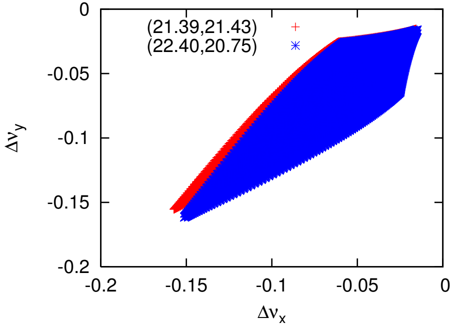

Figure: Tune footprint ($\Delta\nu_{x,y}(J_x, J_y)$) due to space charge force.

Tune slope Space Charge Potential

$$\frac{\partial^2 U_{00}}{\partial J_x^2} = -\frac{\lambda_p r_p}{\beta^2\gamma^3}\oint ds \frac{\beta_x^2}{\sigma_x^4}$$
$$\int_0^\infty \frac{e^{-w_x - w_y} dt}{(2+t)^{5/2}(2r_{yx}+t)^{1/2}} \left[\left\{\frac{3}{2}I_0(w_x) - 2I_1(w_x) + \frac{1}{2}I_2(w_x)\right\} I_0(w_y)\right],$$

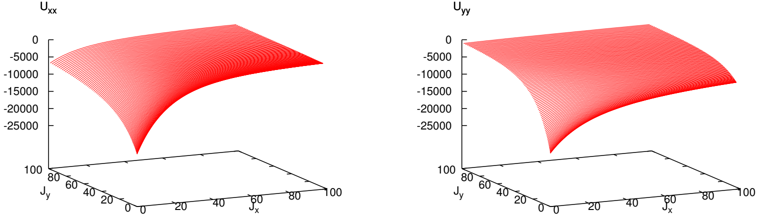

Figure: Tune slope ($U_{ij} = \partial^2 U_{00}/\partial J_i \partial J_j$) due to space charge force.

Resonance terms

$$U_{m_x,m_y}(J_x,J_y) = -\frac{\lambda_p r_p}{\beta^2\gamma^3}\oint ds \int_0^\infty \frac{du}{\sqrt{2\sigma_x^2+u}\sqrt{2\sigma_y^2+u}}$$

$$\left[\delta_{m_x0}\delta_{m_y0} - \exp(-w_{x\eta}-w_y)\sum_{l=-\infty}^{\infty}(-1)^{(m_x+l+m_y)/2}\right.$$

$$\left. I_{(m_x-l)/2}(w_x) I_l(v_x) I_{m_y/2}(w_y) e^{-im_x\varphi_x - im_y\varphi_y}\right]. \quad (18)$$

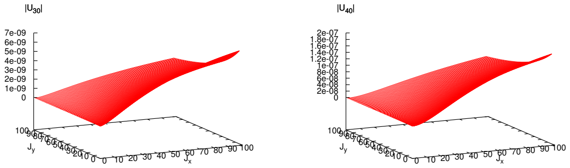

Figure: $U_{30}(\delta = \sigma_\delta)$ and $U_{40}(\delta = 0)$ due to space charge force.

Tune shift due to lattice nonlinearity

One turn map is given by Taylar expansion of lattice elements.

$$
\begin{aligned}
U_{00}(\boldsymbol{J}) &= 3.43103\times10^{14}J_x^6 + 7.36914\times10^{14}J_x^5J_y + 7.17029\times10^{11}J_x^5 + 2.34124\times10^{15}J_x^4J_y^2 \\
&+ 1.70991\times10^{12}J_x^4J_y + 1.43961\times10^{8}J_x^4 + 4.48931\times10^{15}J_x^3J_y^3 + 2.20917\times10^{12}J_x^3J_y^2 \\
&+ 2.50211\times10^{8}J_x^3J_y + 613899.J_x^3 + 3.33998\times10^{15}J_x^2J_y^4 + 1.79716\times10^{12}J_x^2J_y^3 \\
&+ 7.07531\times10^{8}J_x^2J_y^2 + 809323.J_x^2J_y + 1095.71J_x^2 + 7.58773\times10^{14}J_xJ_y^5 \\
&+ 5.7438\times10^{11}J_xJ_y^4 + 4.55828\times10^{8}J_xJ_y^3 + 650655.J_xJ_y^2 + 2096.06J_xJ_y \\
&+ 4.11283\times10^{13}J_y^6 + 4.00294\times10^{10}J_y^5 + 5.3027\times10^{7}J_y^4 + 79924.4J_y^3 + 1106.98J_y^2 \quad .
\end{aligned}
$$

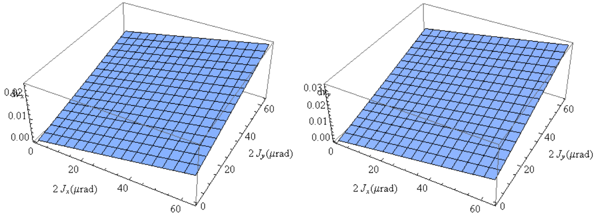

Figure: Tune spread ($\Delta\nu_{x,y}(J_x, J_y)$) due to lattice nonlinearity.

Tune slope due to lattice nonlinearity

Tune slope is given by the one turn map.

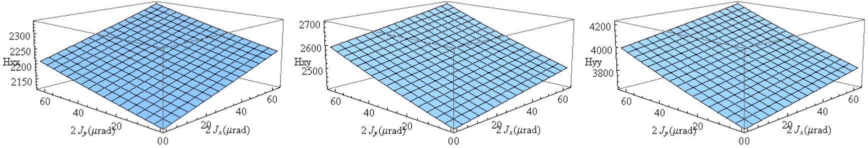

Figure: Tune slope ($\partial^2 H_{00}/\partial J_x^2$, $\partial^2 H_{00}/\partial J_x \partial J_y$ and $\partial^2 H_{00}/\partial J_y^2$) due to lattice nonlinearity.

The tune shift and slope due to lattice nonlinearity are one order smaller than those of space charge.

mx	my	Jx	Jy	|Um| (B0)	|Um| (B)	|Um| (BR)
1	0	3.6E−05	0.0E+00	4.84E−08	1.88E−07	1.86E−07
2	0	3.6E−05	0.0E+00	2.47E−08	4.55E−08	4.66E−08
1	1	1.8E−05	1.8E−05	1.28E−25	1.67E−26	4.01E−09
0	2	0.0E+00	3.6E−05	5.55E−09	3.91E−09	2.69E−09
3	0	3.6E−05	0.0E+00	5.46E−08	1.29E−07	1.32E−07
2	1	1.8E−05	1.8E−05	2.09E−25	1.42E−26	1.42E−07
2	−1	1.8E−05	1.8E−05	2.16E−25	4.52E−27	7.96E−08
1	2	1.8E−05	1.8E−05	4.66E−08	1.78E−07	1.83E−07
1	−2	1.8E−05	1.8E−05	1.48E−07	2.72E−07	2.72E−07
0	3	0.0E+00	3.6E−05	1.42E−25	1.59E−26	1.10E−07
4	0	3.6E−05	0.0E+00	2.50E−07	2.51E−07	2.51E−07
3	1	1.8E−05	1.8E−05	1.93E−26	2.52E−27	6.80E−09
3	−1	1.8E−05	1.8E−05	1.61E−26	4.97E−27	7.04E−10
2	2	1.8E−05	1.8E−05	2.49E−08	5.90E−09	5.58E−09
2	−2	1.8E−05	1.8E−05	1.27E−08	8.40E−09	8.03E−09
1	3	1.8E−05	1.8E−05	2.52E−26	5.66E−27	3.56E−09
1	−3	1.8E−05	1.8E−05	1.63E−26	1.10E−26	8.42E−10
0	4	0.0E+00	3.6E−05	1.20E−08	1.45E−08	1.42E−08

Table: $U_{m_x,m_y}(J)$ for lattice nonlinearity. U's are evaluated at J 3rd and 4-th column. The suffix, B0,B and BR means lattices without errors, lattice with measured beta and measured beta and coupling, K.Ohmi, HB2012.

J-PARC MR ring has superperiodicity of three. Resonances without $m_x\nu_x + m_y\nu_y = 3n$ is suppressed under the perfect superperidicity. It is sufficient to consider 1/3 ring.

$$\mathcal{M} = \left[\exp\left(-H^{(1)}_{00} - H^{(1)}_{\boldsymbol{m}}\right)\right]^3 \tag{19}$$

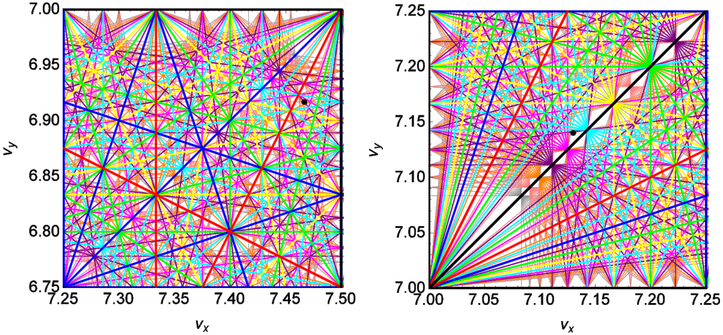

Figure: .Tune diagram near $(\nu_x/3, \nu_y/3) = (7.467, 6.917)$ and $(7.13, 7.143)$.

Resonance terms under superperiodicity 3

New operating point, $(\nu_x, \nu_y) = (21.39, 21.43)$,
$(\nu_x/3, \nu_y/3) = (7.13, 7.143)$,

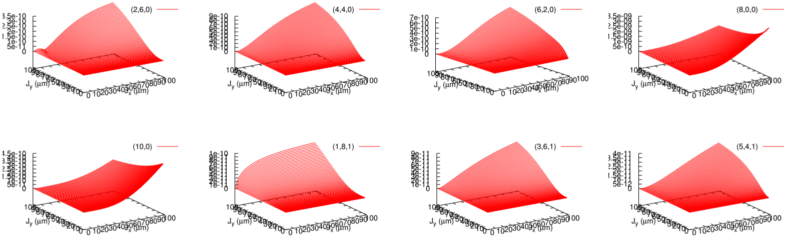

Figure: .Resonance terms near $(\nu_x, \nu_y) = (21.39, 21.43)$

Resonance terms under superperiodicity 3

Present operating point, $(\nu_x, \nu_y) = (22.40, 20.75)$,
$(\nu_x/3, \nu_y/3) = (7.4667, 6.9167)$,

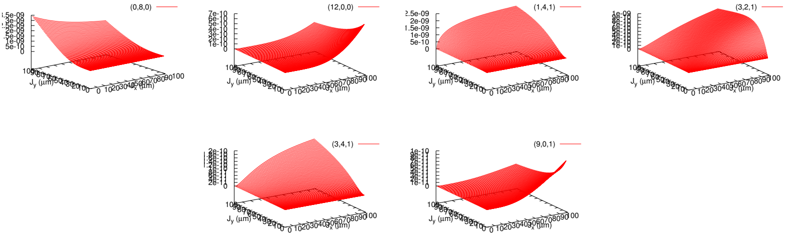

Figure: Resonance terms near $(\nu_x, \nu_y) = (22.40, 20.75)$.

Breaking of Superperiodicity

In real accelerator, superperiodicity is broken by various errors.
Non-structure resonances appear.

$$\mathcal{M} = \exp\left(-H_{00}^{(3)} - H_{\boldsymbol{m}}^{(3)}\right) \exp\left(-H_{00}^{(2)} - H_{\boldsymbol{m}}^{(2)}\right) \exp\left(-H_{00}^{(1)} - H_{\boldsymbol{m}}^{(1)}\right) \quad (20)$$

$$H_{00}^{(2,3)} + H_{\boldsymbol{m}}^{(2,3)} = H_{00}^{(1)} + H_{\boldsymbol{m}}^{(1)} + \Delta H_{00}^{(2,3)} + \Delta H_{\boldsymbol{m}}^{(2,3)} \quad (21)$$

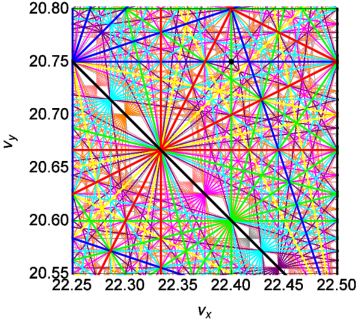

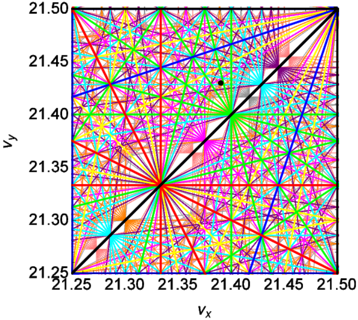

Figure: .Tune diagram near $(\nu_x, \nu_y) = (22.40, 20.75)$ and (21.39, 21.43)

Beta function measurement

Beta function distortion breaks superperiodicity. Beta function and phase are measured by turn-by-turn monitor (and/or orbit response).
x_1, x_2 : turn-by-turn positions of monitor 1 and 2, m_{ij}: transfer matrix between 1 and 2.

$$\begin{pmatrix} x_1' \\ x_2' \end{pmatrix} = \frac{1}{m_{12}} \begin{pmatrix} -m_{11} & 1 \\ -1 & m_{22} \end{pmatrix} \begin{pmatrix} x_1 \\ x_2 \end{pmatrix} \tag{22}$$

turn average of phase space position for x mode excitation

$$\begin{pmatrix} \beta_x \\ \alpha_x \end{pmatrix}_1 = \frac{1}{\sqrt{\langle x_1^2 \rangle \langle x_1'^2 \rangle - \langle x_1 x_1' \rangle^2}} \begin{pmatrix} \langle x_1^2 \rangle \\ -\langle x_1 x_1' \rangle \end{pmatrix} \tag{23}$$

Betatron phase difference

$$\cos(\phi_{x,2} - \phi_{x,1}) = \frac{\langle x_1 x_2 \rangle}{\sqrt{\langle x_1^2 \rangle \langle x_2^2 \rangle}} \tag{24}$$

Measured beta function and phase

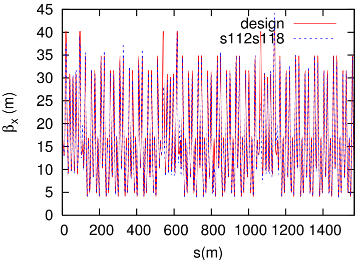

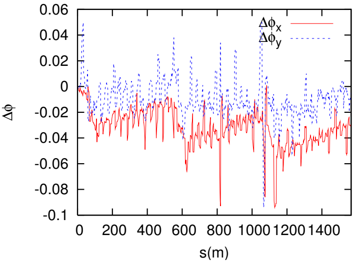

Figure: Measured beta function and phase for shot 112 (x) and 118 (y).

Space charge induced resonances with measured beta

Integration along s in Eq.(18) is performed using measured beta and phase.

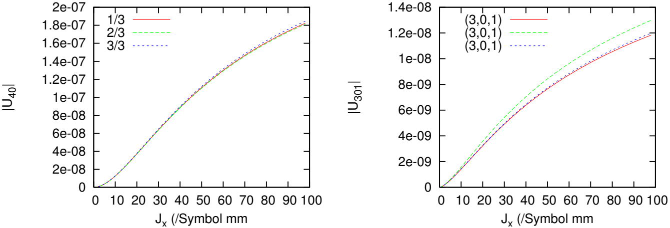

Figure: U_{301} and U_{40} for space charge force given by measured beta function and phase.

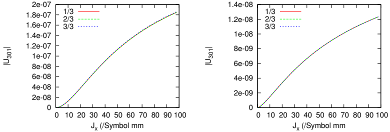

Figure: U_{301} and U_{40} for space charge force in the design lattice.

Lattice magnets induced resonances with measured beta

Lattice nonlinearity is factorized in each super period (SUP).

$$\mathcal{M}^{(sup)} = \prod_{i=0}^{N-1} M(s_{i+1}, s_i) e^{-:H_I(s_i):} = exp\left(-H_{00}^{(sup)} - H_{\boldsymbol{m}}^{(sup)}\right), \qquad (25)$$

$$\begin{aligned} M(s_{i+1}, s_i) &= V^{-1}(s_{i+1}) U_{i+1,i} \Delta U_i V(s_i) \qquad (26) \\ &= V^{-1}(s_{i+1}) V_0(s_{i+1}) M_0(s_{i+1}, s_i) V_0^{-1}(s_i) \Delta U_i V(s_i) \end{aligned}$$

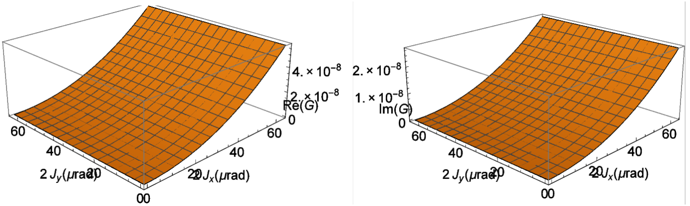

Figure: Real and imaginary part of H_{40} for lattice nonlinearity in first SUP. Measured beta and phase are contained in V and ΔU in Eq.(26).

Integration of the resonance Hamiltonian

Simulation for emittance growth can be done using the resonance (Fourier expanded) Hamiltonian.

$$H = \mu_x J_x + \mu_y J_y + U_0(J_x, J_y) \\ +U_{m,c}(J_x, J_y)\cos m\phi + U_{m,s}(J_x, J_y)\sin m\phi. \quad (27)$$

where $m\phi = m_x\phi_x + m_y\phi_y$.
Symplectic transformation for above Hamiltonian is expressed by

$$\begin{aligned} \bar{\phi}_i &= \phi_i + \frac{\partial U_0}{\partial J_i} + \frac{\partial U_{m,c}}{\partial J_i}\cos m\phi - \frac{\partial U_{m,s}}{\partial J_i}\sin m\phi \\ J_i &= \bar{J}_i - m_i(U_{m,c}\sin m\phi - U_{m,s}\cos m\phi). \end{aligned} \quad (28)$$

where $\bar{J}$ and $\bar{\phi}$ are those after the transformation, and U_m's are function of $\bar{J}_i$ and ϕ_i. Second equation of Eq.(28) is implicit relation.

Simulation without synchrotron motion

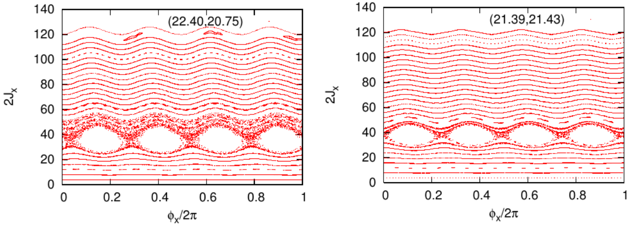

Figure: Phase space trajectory for the model map with U_{40}. No synchrotron motion. Left and right plots correspond to tune (22.40,20.75) and (21.39,21.43), respectively.

Analytical estimate of the resonance width agrees well

$$\Delta J_x = 4\sqrt{\frac{U_m}{\partial^2 U_{00}/\partial J_x^2}} = 4\sqrt{\frac{10^{-7}}{10^4}} = 12\times 10^{-6}\mathrm{m} = 12\mu\mathrm{m} \qquad (29)$$

Simulation with synchrotron motion

Beam charge density depends on z. The resonance structure modulates due to synchrotron oscillation.

$$\lambda(z,s) = \frac{N_p}{\sqrt{2\pi}\sigma_z}\exp\left(-\frac{z(s)^2}{2\sigma_z^2}\right) \tag{30}$$

$$z = z_0\cos(\mu_s s/L) = z_0\cos(\mu_s n_{turn}) \tag{31}$$

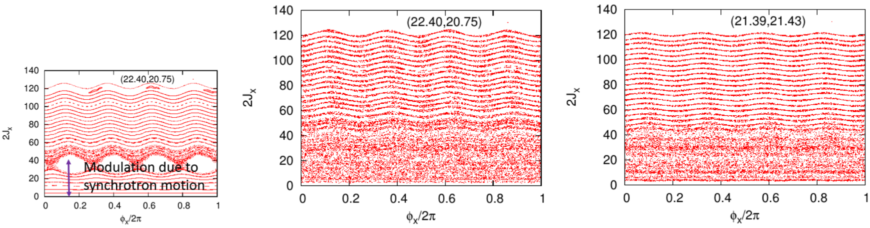

Figure: Phase space trajectory for the model map with U_{40}. Synchrotron tune, $\nu_s = 0.002$, $z_0 = \sigma_z$. Left and right plots correspond to tune (22.40,20.75) and (21.39,21.43), respectively

Emittance growth, diffusion of J

Initializing $\delta(\boldsymbol{J}-\boldsymbol{J}_0)$, uniform ϕ, calculate evolution of spread of $\boldsymbol{J}$.

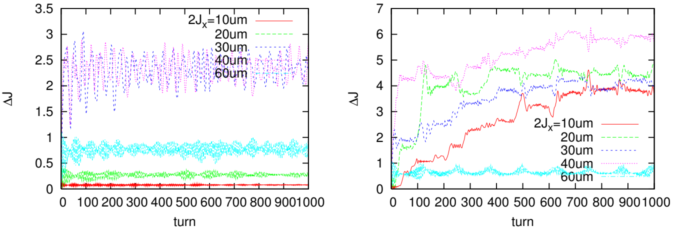

Figure: Diffusion of J. Left is for no synchrotron moiton. Right is for Synchrotron tune, $\nu_s = 0.002$, $z_0 = \sigma_z$.

Diffusion of J with synchrotron motion is larger than those without synchrotron motion. All particles $J_x < 40\mu$m diffuse for finite ν_s, while limited particles $J_x = 30$ and 40 have large ΔJ, but not diffusive.

Simulation under broken superperiodicity using measured beta

Preliminary, only space charge resonances are taken into account.
Very clean phase space. Probably, this result is too clean compare with beam loss experience in J-PARC MR. Resonances due to lattice nonlinearity may dominate.

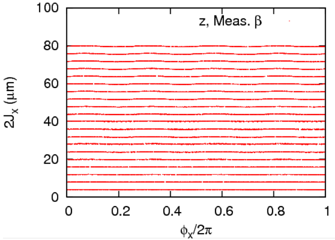

Figure: .Phase space trajectory for the model map based on measured beta.

Summary

- Emittance growth based on chaos near resonances is discussed.
- Tune shift and slope for space charge and lattice is evaluated.
- Resonance terms for space charge and lattice is evaluated.
- Beta function, phase and x-y coupling have been measured in J-PARC MR turn by turn monitors.
- Resonance terms are evaluated by the measured beta and phase.
- Resonance fixed point and width are determined by the tune slope and resonance strength.
- Simulation of a model based on the tune slope and resonance strength is being performed.
- Emittance growth is evaluated by combination with Synchrotron motion
- The results are preiminary yet for the emittance growth based on measured beta.
- Simulations for Multi-resonances will be performed.

The End

Thank you for your attention

Canonical Transformation to Resonance base

Generating function for the canonical transformation

$$F_2(\boldsymbol{P},\phi) = (J_{x,R} + m_x P_1 + m_{x,2} P_2)\phi_x + (J_{y,R} + m_y P_1 + m_{y,2} P_2)\phi_y \quad (32)$$

Resonance base (choose $m_{x,2} = 0$, $m_{y,2} = 1$)

$$P_1 = \frac{J_x - J_{x,R}}{m_x} \qquad \psi_1 = m_x \phi_x + m_y \phi_y \quad (33)$$

$$P_2 = (J_y - J_{y,R}) - \frac{m_y}{m_x}(J_x - J_{x,R}) \qquad \psi_2 = \phi_y$$

Hamiltonian, U_{00}

$$U_{00} \approx \frac{\Lambda}{2} P_1^2 \qquad \Lambda = m_x^2 \frac{\partial^2 U_{00}}{\partial J_x^2} + m_x m_y \frac{\partial^2 U_{00}}{\partial J_x \partial J_y} + m_y^2 \frac{\partial^2 U_{00}}{\partial J_y^2} \quad (34)$$

Newton Raphson method for Symplectic integration

To solve $(\bar{J}, \bar{\phi})$, Newton-Raphson method is used.

$$f_x = \bar{J}_x - J_x - m_x(U_{m,c} \sin m\phi - U_{m,s} \cos m\phi) = 0$$

$$f_y = \bar{J}_y - J_y - m_y(U_{m,c} \sin m\phi - U_{m,s} \cos m\phi) = 0. \qquad (35)$$

Iteration of Newton method is expressed by

$$\begin{pmatrix} \bar{J}_x \\ \bar{J}_y \end{pmatrix}_{n+1} = \begin{pmatrix} \bar{J}_x \\ \bar{J}_y \end{pmatrix}_n - F^{-1} \begin{pmatrix} f_x \\ f_y \end{pmatrix}_n . \qquad (36)$$

where F is Jacobian matrix for f_i; $F_{ij} = \partial f_i / \partial J_j$, $i, j = x, y$.